



ARL-TR-9186 • APR 2021



Preliminary Investigation into Thermal and Mechanical Properties of Ionically Cross-linked Cellulose Nanofibril Films

by Eugene Napadensky, Joshua A Orlicki, James F Snyder, Alda Kapllani, and Hong Dong

Approved for public release: distribution unlimited.

NOTICES

Disclaimers

The findings in this report are not to be construed as an official Department of the Army position unless so designated by other authorized documents.

Citation of manufacturer's or trade names does not constitute an official endorsement or approval of the use thereof.

Destroy this report when it is no longer needed. Do not return it to the originator.



Preliminary Investigation into Thermal and Mechanical Properties of Ionically Cross-linked Cellulose Nanofibril Films

Eugene Napadensky, Joshua A Orlicki, James F Snyder, and Hong Dong
*Weapons and Materials Research Directorate,
DEVCOM Army Research Laboratory*

Alda Kapllani
Oak Ridge Institute for Science and Education

REPORT DOCUMENTATION PAGE

Form Approved
OMB No. 0704-0188

Public reporting burden for this collection of information is estimated to average 1 hour per response, including the time for reviewing instructions, searching existing data sources, gathering and maintaining the data needed, and completing and reviewing the collection information. Send comments regarding this burden estimate or any other aspect of this collection of information, including suggestions for reducing the burden, to Department of Defense, Washington Headquarters Services, Directorate for Information Operations and Reports (0704-0188), 1215 Jefferson Davis Highway, Suite 1204, Arlington, VA 22202-4302. Respondents should be aware that notwithstanding any other provision of law, no person shall be subject to any penalty for failing to comply with a collection of information if it does not display a currently valid OMB control number.

PLEASE DO NOT RETURN YOUR FORM TO THE ABOVE ADDRESS.

1. REPORT DATE (DD-MM-YYYY) April 2021		2. REPORT TYPE Technical Report		3. DATES COVERED (From - To) 1 June 2013–1 March 2015	
4. TITLE AND SUBTITLE Preliminary Investigation into Thermal and Mechanical Properties of Ionically Cross-linked Cellulose Nanofibril Films				5a. CONTRACT NUMBER	
				5b. GRANT NUMBER	
				5c. PROGRAM ELEMENT NUMBER	
6. AUTHOR(S) Eugene Napadensky, Joshua A Orlicki, James F Snyder, Alda Kapllani, and Hong Dong				5d. PROJECT NUMBER	
				5e. TASK NUMBER	
				5f. WORK UNIT NUMBER	
7. PERFORMING ORGANIZATION NAME(S) AND ADDRESS(ES) DEVCOM Army Research Laboratory ATTN: FCDD-RLW-MG Aberdeen Proving Ground, MD 21005				8. PERFORMING ORGANIZATION REPORT NUMBER ARL-TR-9186	
9. SPONSORING/MONITORING AGENCY NAME(S) AND ADDRESS(ES)				10. SPONSOR/MONITOR'S ACRONYM(S)	
				11. SPONSOR/MONITOR'S REPORT NUMBER(S)	
12. DISTRIBUTION/AVAILABILITY STATEMENT Approved for public release: distribution unlimited.					
13. SUPPLEMENTARY NOTES ORCID ID(s): Eugene Napadensky, 0000-0002-2021-0254; Joshua A Orlicki, 0000-0001-8522-0034; Hong Dong, 0000-0002-0538-2525					
14. ABSTRACT This work describes the manufacturing process of optically clear films from cellulose nanofibril (CNF) materials, as well as sequential exchange of Na ions present in CNF with a variety of different metallic ions—Al, Fe, Ba, Cu, Zn—in an attempt to improve mechanical properties. Successful substitution of a Na ion in starting material was verified by use of X-ray photoelectron spectroscopy. Effects of ion exchange/cross-linking on the films were evaluated using thermogravimetric analysis and tensile-strength measurements. It was shown that tensile strength and toughness increase when divalent cations are used for exchange (Ba, Cu, Zn), while exchanging sodium for trivalent cations (Al, Fe) produces detrimental effects on films' mechanical properties.					
15. SUBJECT TERMS cellulose nanofibril, CNF, film casting, ion exchange, mechanical properties, Fourier transform infrared spectroscopy, FTIR, X-ray photoelectron spectroscopy, XPS, thermogravimetric analysis, TGA, ionic cross-links					
16. SECURITY CLASSIFICATION OF:			17. LIMITATION OF ABSTRACT UU	18. NUMBER OF PAGES 28	19a. NAME OF RESPONSIBLE PERSON Eugene Napadensky
a. REPORT Unclassified	b. ABSTRACT Unclassified	c. THIS PAGE Unclassified			19b. TELEPHONE NUMBER (include area code) (410) 306-0682

Contents

List of Figures	iv
List of Tables	iv
1. Introduction	1
2. Experimental	2
2.1 Materials	2
2.2 Film Preparation and Exchange	2
2.3 Evaluation Techniques	5
2.3.1 TGA	5
2.3.2 Fourier Transform Infrared Spectroscopy (FTIR) Analysis	6
2.3.3 XPS Analysis	6
2.3.4 Tensile-Strength Analysis	7
3. Results and Discussion	7
3.1 TGA Results	7
3.2 FTIR Results	8
3.3 XPS Results	11
3.4 Mechanical Properties	12
4. Conclusions	15
5. References	17
Appendix. Relative Signal Intensities	19
List of Symbols, Abbreviations, and Acronyms	21
Distribution List	22

List of Figures

Fig. 1	Graphical representation of H-bonded polysaccharide chains stacking together into CNCs	1
Fig. 2	Chemical structure of CNF repeat unit	3
Fig. 3	Schematic representation of ion exchange/cross-linking procedure for CNF films using chloride salt solutions.....	4
Fig. 4	Color and clarity of various CNF films on white background; black label representing type of film is printed on paper underneath the films	5
Fig. 5	Thermogravimetric plots for various samples showing wt% loss as function of temperature (a) and their derivatives (b).....	8
Fig. 6	Full-range FTIR spectra of evaluated salt-exchanged cellulose samples.....	8
Fig. 7	FTIR spectra of evaluated salt-exchanged cellulose samples zoomed to 1800 to 1200 cm^{-1} region.....	9
Fig. 8	Selected XPS spectra of regions associated with metals of interest ...	12
Fig. 9	Bar-graph representation of mechanical data. Metal valence is color-coded as blue = +1, green = +2, and red = +3.	14

List of Tables

Table 1	Wavenumbers summary of peaks observed in the FTIR spectra.....	10
Table 2	Mechanical test results	13
Table A-1	Relative atomistic concentration of various ion-exchanged cellulose nanofibril (CNF) membranes calculated based on average of collected X-ray photoelectron spectroscopy runs	20

1. Introduction

Cellulose is a naturally occurring polysaccharide obtained from wood and a variety of plants. Depending on the sources of raw materials and specific processes by which this material is purified from the wood pulp, the resulting product can be classified into various types of insoluble particles, including cellulose microfibrils (CMFs), nanofibrils (CNFs), and nanocrystals (CNCs). Each possesses somewhat different properties due to differences in particle size, aspect ratios, and crystalline nature; however, they all possess high levels of hydroxyl groups on the surface.¹⁻⁴

Cellulose is composed of highly aligned individual polysaccharide chains that are extensively hydrogen (H) bonded^{3,5-8} to form flat sheets, which can further stack through interplane H bonding to form high-aspect ratio crystals (Fig. 1). Very-high axial stiffness of these bio-derived and renewable fibers/crystals makes them potentially viable as a reinforcing material for nanocomposites.^{2,4,7,9} In addition to providing structural reinforcement, cellulose-based composites can be made optically transparent,^{7,9,10} making them of broad interest to the US Army as a potential component in transparent composites. However, there are a number of impediments to optimal fabrication of nanocellulose-reinforced materials. Besides the potential application as fillers, another example of potential utility is exploring the use of freestanding cellulose films as interlayers in laminate composites.

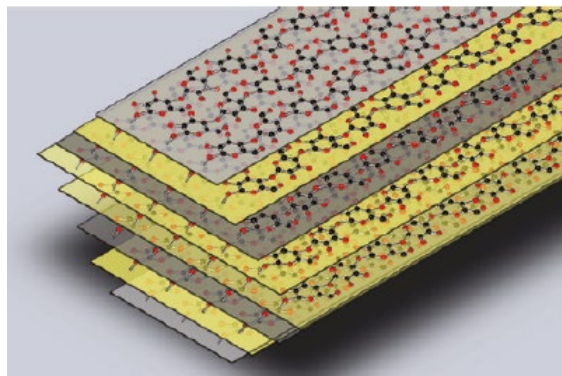


Fig. 1 Graphical representation of H-bonded polysaccharide chains stacking together into CNCs (reprinted with permission from Li and Rennekar⁵ [2011], American Chemical Society)

This report focuses on determining the mechanical properties of freestanding films formed from one of the cellulose types and exploring the ability to improve the properties by creating metal-ion cross-links within the films. Cellulose nanomaterials selected for this work are CNFs manufactured by enzymatic hydrolysis at the US Department of Agriculture's (USDA's) Forest Product Laboratory. It consists of a large quantity of crystalline regions (~70%) connected

by amorphous fibrils, resulting in high-aspect ratio whiskers (few microns by 3–5 nm).^{5,6,9} This material can be formed into thin transparent films^{7,9,10} by solvent casting. As a byproduct of manufacturing, the surface of the whiskers contains sodium (Na)-neutralized carboxylic acid. A variety of divalent and trivalent metal ions will be used to replace the Na cation and cross-link the individual particles, potentially resulting in a more mechanically robust system that will be compared to original films. A certain degree of characterization will also be performed such as X-ray photoelectron spectroscopy (XPS) to verify incorporation of the new ions into the film, thermogravimetric analysis (TGA) to verify retention of thermal stability, and tensile testing to evaluate changes in mechanical properties.

2. Experimental

2.1 Materials

The following materials were used in obtaining experimental data for this report:

- CNFs “2012–FPL–CNF–052–A, 1.3-mmol COONa form”, containing medium-high levels of CNCs (~70%) and obtained from the USDA Forest Product Laboratory. It was received as a solid suspended in water—approximately 1 wt%.

In addition to cellulose, the following chemicals were used as received, without further purification:

- Deionized water (Sigma-Aldrich, high-performance liquid chromatography [HPLC] grade), methanol (Sigma-Aldrich, ReagentPlus grade, 99.8%), aluminum chloride 6-hydrate (J.T.Baker), ferric chloride (EM Science, anhydrous, 98%), barium chloride (J.T.Baker, anhydrous), copper (II) chloride dehydrate (Acros Organics, 99%), and zinc chloride (EM Science, anhydrous, 98%).

2.2 Film Preparation and Exchange

The chemical structure of the particular cellulose nanomaterial selected for this work is shown in Fig. 2.

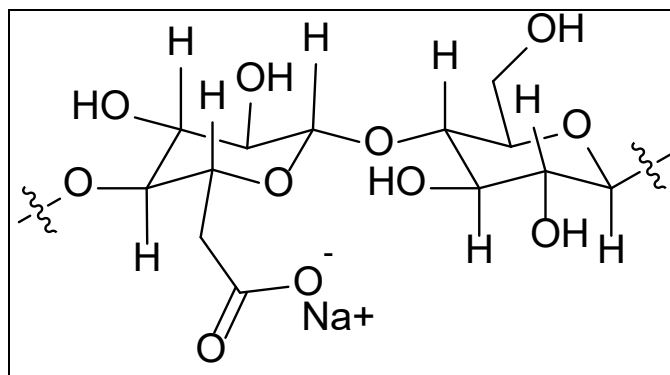


Fig. 2 Chemical structure of CNF repeat unit

It is expected that when the evaluated metal ions replace existing Na ions present on the surface of nanofibrils as part of the neutralized carboxylic acid groups, they will, at least in some cases, create ionic cross-links between different fibrils. It was previously shown that adding metal ions to dilute solution of the CNF results in rapid formation of an insoluble gel.^{6,10} In this work, cross-linking will be attempted on swollen films and mobility of individual CNF particles will be highly restricted. This may limit the diffusion of metal ions to sites that are susceptible to collation with the metal ions, as well as availability of additional neighboring groups to complete the cross-linking process. While freestanding films produced by solvent-casting CNF solutions are not soluble in water, they do tend to swell and appear noticeably weaker in strength. This indicates increased levels of mobility of individual crystals. It is expected that this increase of mobility will be sufficient for the metal ions to find good receptor sites resulting in strong ionic cross-links between different fibrils. The most obvious location of this reaction would be the Na carboxylic group; however, it is possible that some of the hydroxyl groups would also precipitate by metal chelation to increase possibility of successful cross-linking. The cross-linking reaction is expected to occur only on the surface of the crystals/fibrils since the stacked layers of polysaccharide sheets are tightly held by van der Waals forces^{3,5} and interlayer H bonds that prevent any ions from diffusing into the interior.

For this study, five different metal ions were chosen: Al^{3+} , Fe^{3+} , Ba^{2+} , Cu^{2+} , and Zn^{2+} . They were selected to provide a somewhat extensive range of properties such as valence, electronegativity, and atomic radius. In addition, the original CNF was evaluated, which was provided in a Na form and will be serving as a baseline material to which the modified ones will be compared.

The CNF/water suspension supplied by the manufacturer contained roughly 1% solids by weight and was diluted with methanol, creating a 90% water/10% methanol solvent to improve viscosity and flow. Freestanding films were solvent-

cast directly from this solution by using a “doctor blade” method on a polycarbonate surface. The height on the blade was set to 4 mm and after drying 4–5 days at atmospheric conditions, this resulted in 0.015- to 0.02-mm-thick transparent films.

The ion-exchange procedure, shown schematically in Fig. 3, consisted of submerging freestanding CNF films into a 0.5-M molar salt solution of the corresponding salt: AlCl_3 , FeCl_3 , BaCl_2 , CuCl_2 , or ZnCl_2 . Films would rapidly swell and become very flexible, and after allowing 1 h for ions to diffuse into the bulk of the material and form ionic bonds to the nanocrystals, films were removed from solution. They were rinsed in deionized water and then soaked in a fresh water bath for 30 min to allow unbonded ions to diffuse from the film. Water was replaced and films were soaked for an additional 30 min. When washing away unbonded ions was complete, as later verified by XPS analysis, films were moved into a methanol bath to dehydrate. Drying CNF films soaked with water (ion exchanged or otherwise) proved very difficult due to the high levels of swelling and drying defects. Very often the drying process produced wrinkles and internal stresses that resulted in films that were no longer flat and not very appropriate for tensile-strength experiments. Dehydration in methanol for 5 min results in films that are already shrunken but not too brittle to work with. They can be placed between two sheets of paper and air-dried under light weight for 1–2 h. After exchange with metal salts, the films remained transparent but there was a color change associated with two of the salts used in the experiment. Films exchanged with CuCl_2 acquired a slight blue tint, and films exchanged with FeCl_3 turned amber color (Fig. 4). The same color changes were observed in formation of freestanding CNF gels when exposed to corresponding ions.⁶

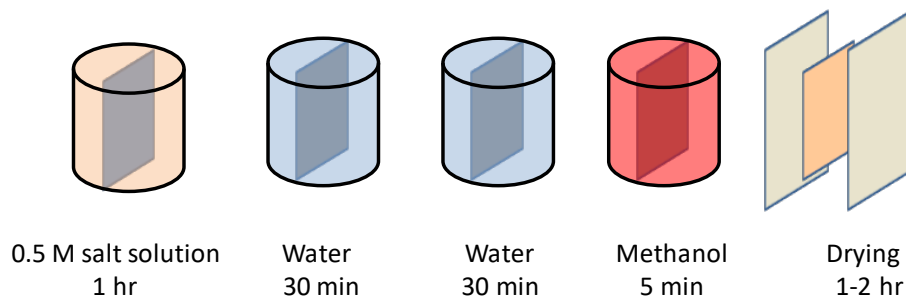


Fig. 3 Schematic representation of ion exchange/cross-linking procedure for CNF films using chloride salt solutions

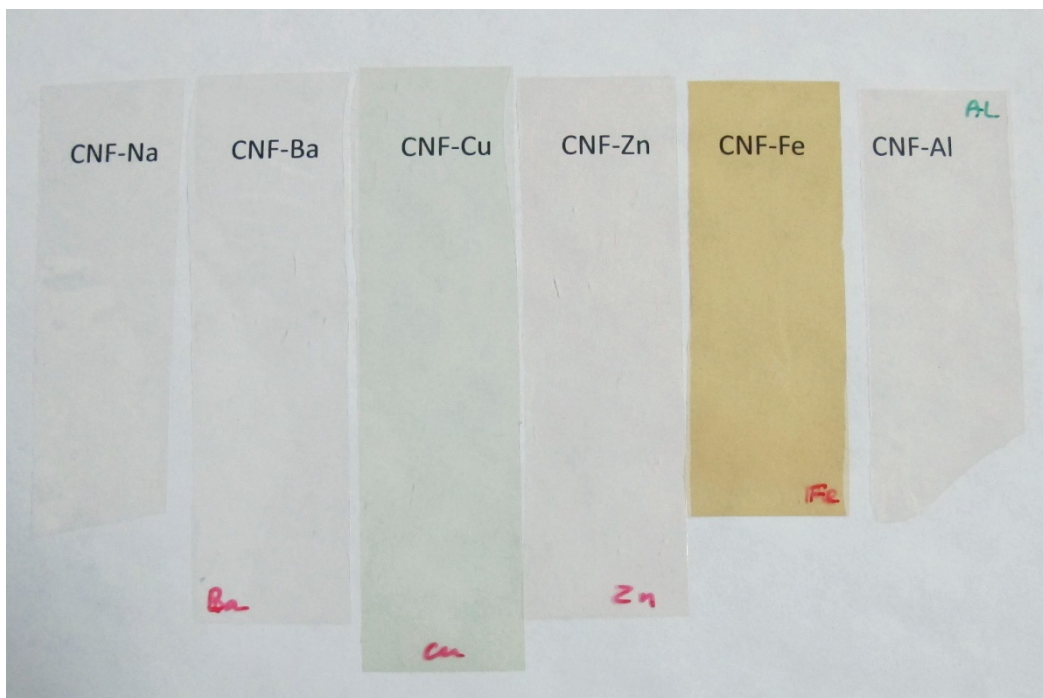


Fig. 4 Color and clarity of various CNF films on white background; black label representing type of film is printed on paper underneath the films

After films were dried, they were cut into thin strips 90 to 110 mm in length. A few different techniques were attempted and the one that produced the best results (strips with evenly cut parallel edges and minimal defects such as nicks and cuts) was obtained by using a large paper cutter. CNF films were placed between two sheets of paper and then cut to a width of 25.4 or 12.7 mm. Samples exchanged with certain ions that were cut with a width of 25.4 mm proved too strong for the load cell equipped on the instrument. A maximum load of 50 N was reached without the samples breaking. To provide meaningful results, narrower films were cut for tensile experiments—thus the appearance of the 12.7-mm geometries for some of the samples. The differences in cross section due to the change of geometry was taken into account when all applicable calculations were made.

2.3 Evaluation Techniques

2.3.1 TGA

The TGA technique was used to evaluate thermal decomposition properties of the metal-ion-exchanged CNF films and compare them to the original (Na salt) material. The TGA instrument used for this work was model Q5000-IR manufactured by TA Instruments and uses a nitrogen gas purge. TGA involves heating up a small piece of material in a controlled fashion, typically in an air or

nitrogen atmosphere. As the temperature increases and material thermally decomposes (if nitrogen atmosphere is used) or oxidizes (if air atmosphere is used), small decreases in weight are recorded using a built-in supersensitive balance. This technique provides investigators with information regarding thermal stability of the material as well as insight into sample purity and changes in chemical structure.

Testing was done using 5–8 mg of the sample, according to manufacturer's recommendations. They were analyzed under nitrogen purge in platinum pans using the following temperature programming: equilibrate at 35 °C and then ramp to 700 °C at a rate of 10 °C per min.

2.3.2 Fourier Transform Infrared Spectroscopy (FTIR) Analysis

FTIR spectra were obtained using a Nicolet iS50 spectrometer from Thermo Fisher Scientific. Data for polymer films were obtained using the integrated attenuated total reflectance fixture, employing a single-bounce beam path with a diamond crystal. At least 64 scans were acquired with a minimum resolution of 4 cm⁻¹. Once acquired, the spectra were compared to an internal library of general and polymeric materials, as well as tables of functional group chemical shifts.¹¹

2.3.3 XPS Analysis

XPS data were acquired with a Physical Electronics Inc (PHI) 5000 VersaProbe II photoelectron spectrometer by using an Al K α X-ray-source base pressure of 1.0×10^{-8} Torr. XPS measures X-ray-generated photoelectrons, providing elemental- and chemical-oxidation state information. The measured photoelectrons escape from the top 10–12 nm of the film, limiting the depth of observation for XPS measurements. All elements except H and He can be detected. The quantitative results are expressed in terms of atomic-percent (at.%) concentrations. Care should be taken when comparing at.% to the more commonly considered wt% and mol%. Atomic percentages from XPS neglect H in the sample, so this caveat must be considered as the data are reviewed. Instrument settings were 200 μ m–50 W–15 kV, referring to spot size, source power, and bias to the filament. Survey (overall) spectra were collected over a range of 0- to 1100-eV binding energy, using 117.4-eV pass energy with a 1-eV step and 10 sweeps. High-resolution data were collected at 23.5-eV pass energy with a 0.05-eV step with 10 sweeps for carbon/oxygen/nitrogen and 30 sweeps for metals. Each film was analyzed in three different spots in an attempt to acquire more representative results.

2.3.4 Tensile-Strength Analysis

Tensile strength of original and metal-ion exchanged films were obtained using an MTS Synergie Electromechanical Universal Test System load frame equipped with a 50-N load cell. The instrument was controlled by TestWorks 4.11 software (MTS Systems Corporation) and most of the data analysis (except where noted) was performed using the same software. To use the same 50-N load frame for analysis of all the samples, sample geometry for films exchanged with certain ions had to be altered. Originally the plan was to use 25.4-mm-wide samples; however, certain samples would not break before the load cell reached the maximum load of 50 N. Ba-, Zn-, and Cu-exchanged films exhibited this behavior; so to test them, specimens half the original width of 12.7 mm were made. The other parameters remained the same: thickness of 18–24 microns and length 80–100 mm. This difference in geometry was accounted for in the calculations. To perform the test, individual specimen thickness was measured and the specimen was clamped in grips spaced 50-mm apart and pulled at a rate of 5 mm/min while collecting data at a 10-Hz acquisition rate. For each sample, about 20–25 specimens were analyzed and after unsuccessful results (operator errors, specimen slipped from grips, specimen damaged during initial loading, specimen broke at grips, etc.) were thrown out, 15–20 useful data sets were obtained for each different metal type. Collected data were analyzed using TestWorks 4.11 software to determine mechanical properties.

3. Results and Discussion

3.1 TGA Results

Due to its nonhomogeneous nature, CNFs exhibit a very complex thermal decomposition profile. The amorphous region, bulk nanocrystals, and the unique functional groups on the surface of the crystals all affect the decomposition temperature to a certain degree. This can be illustrated by examining TGA curves shown in Fig. 5, with 5a showing weight-loss percent and 5b showing the derivative. The black curve labeled “CNF” represents the original unmodified (Na salt) material. It exhibits unusually sharp initial decomposition weight loss, sometimes attributed to thermal decomposition of oxygen-containing functional groups and subsequent loss of CO₂¹² as compared to the more common gradual weight loss seen in all the films that were modified. This rate difference can be explained by the stabilizing effect of cross-linking ions. Other than small (5%–10%) weight loss below 100 °C (assigned to remaining moisture), all decomposition peaks are too complex to resolve. While all samples (with the exception of Al) show a broader main decomposition, the onset of decomposition

still starts at roughly 200 °C. However, the cross-linking of CNF films with various ions did not result in detrimental effects on the thermal stability of the CNF films. What is interesting, however, is that with the exception of CNF–Fe and CNF–Zn (brown and green curves, respectively), all show the presence of different peaks, indicating very involved and complex interaction between the ions and the cellulose.

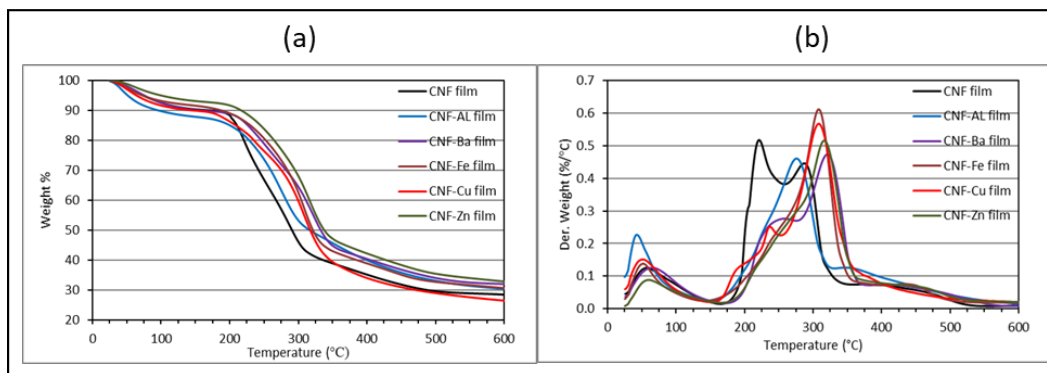


Fig. 5 Thermogravimetric plots for various samples showing wt% loss as function of temperature (a) and their derivatives (b)

3.2 FTIR Results

Full FTIR spectra of the analyzed films are shown in Fig. 6, with specific zoomed-in regions of 1200 to 1800 cm^{-1} wavenumbers in Fig. 7.

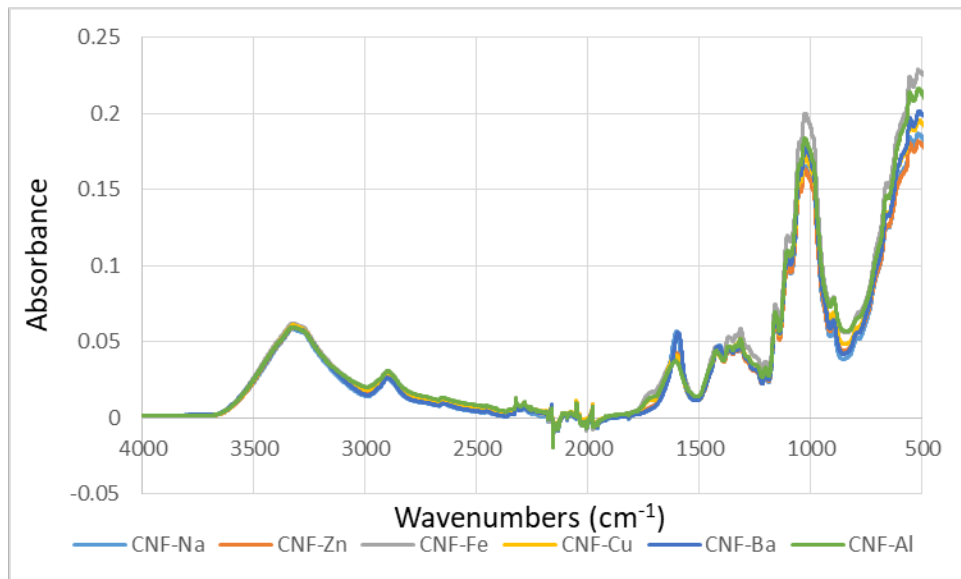


Fig. 6 Full-range FTIR spectra of evaluated salt-exchanged cellulose samples

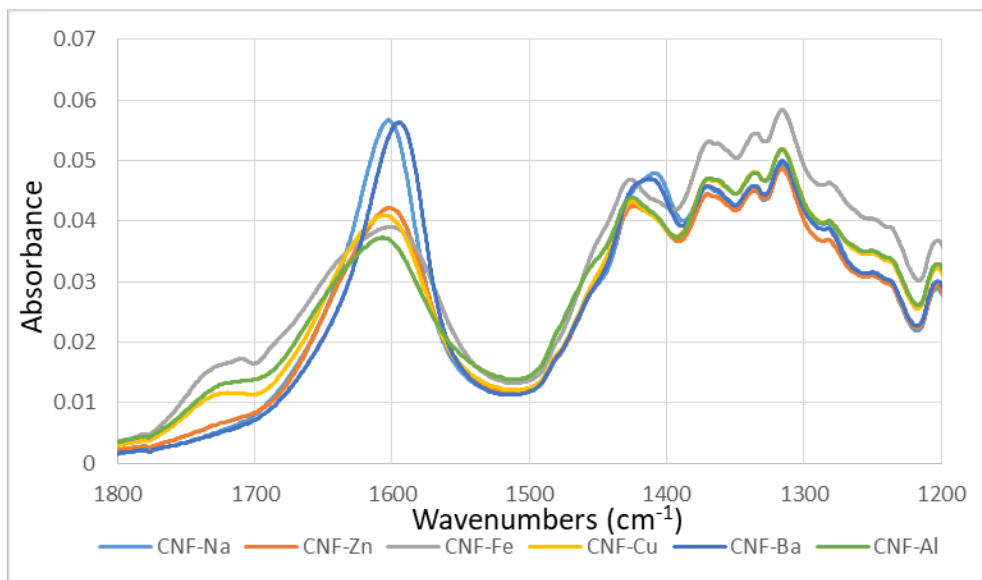


Fig. 7 FTIR spectra of evaluated salt-exchanged cellulose samples zoomed to 1800 to 1200 cm^{-1} region

Analysis of the carbonyl region in the spectra of the original Na salt film clearly shows the strong asymmetric (ν_{as}) stretch peak of the C=O at 1602 cm^{-1} , and has no free acid evident ($1725\text{--}1715 \text{ cm}^{-1}$). Taking the Na salt as a baseline value, the other salts all show similar signals in the region for the carboxylate bonded to the corresponding cation. The expected complementary resonance, the symmetric stretch (ν_{s}), is also observed in the region of $1425\text{--}1408 \text{ cm}^{-1}$ and shows corresponding minor shifts as a function of the cation.¹³ It is interesting that three of the cations, including Fe^{2+} , Cu^{2+} , and Al^{3+} , also showed increased intensity in the range of $1720\text{--}1710 \text{ cm}^{-1}$. Peaks in this range are consistent with signals associated with the free acid (COOH)¹⁴ and may be indicative of some buffering of the solution occurring as the cations were exchanged with the CNF hydrogel. Wavenumbers summary of observed peaks is shown in Table 1.

Table 1 Wavenumbers summary of peaks observed in the FTIR spectra

Sample	Peaks of interest (cm⁻¹)											
CNF-Na	...	1602.6	1408.7	1370.5	1336.3	1315.1	1202.7	1158.6	1105.3	...	1024.8	897.6
CNF-Zn	...	1602.4	1424.2	1369.9	1335.9	1316.3	1202.7	1159.5	1105.2	1051.4	1024.4	897.0
CNF-Fe	1709.3	1602.8	1426.8	1368.9	1334.9	1316.0	1202.5	1159.1	1103.9	1051.0	1025.9	897.9
CNF-Cu	1711.6	1605.8	1424.9	1369.8	1335.6	1316.0	1202.9	1159.5	1104.6	1050.5	1025.8	897.1
CNF-Ba	...	1594.8	1411.7	1370.2	1335.5	1315.9	1202.5	1158.7	1105.5	...	1023.4	897.5
CNF-Al	1709.8	1607.0	1425.1	1369.2	1335.2	1316.1	1202.2	1159.3	1050.5	...	1026.0	897.3

3.3 XPS Results

The motivation to evaluate the CNF films by XPS was threefold. The technique provides measurements to verify the exchange of Na ions by monitoring disappearance of the appropriate peak absorbing at 1072-eV binding energy, to verify appearance of peaks related to new ions, and to confirm the lack of chloride (e.g., unbound salt, appearing at a binding energy of 198.5 eV) in all samples. While the importance of the first two is self-explanatory, monitoring the absorption region for the chloride peak may need some explanation. Even though membranes were thoroughly washed in deionized water to remove unreacted salts, some concerns were raised that the mere presence of a new metal's peak may not truly indicate the new ion is associated with the cellulose, as opposed to existing in chloride salt form mechanically trapped within the membrane. Lack of signal at 198.5-eV binding energy, however, would indicate lack of the counterion chloride in the sample and provide additional indication that any metal ions observed are present as counterions associated with the native carboxylate side chains and not in form of chlorinated salt.

Evaluation of the XPS spectra at binding energies corresponding to metal ions of interest (1072 eV for Na, 73 eV for Al, 707 eV for Fe, 933 eV for Cu, 781 eV for Ba, and 1022 eV for Zn) indicate the presence of the anticipated ions in each corresponding sample (Fig. 8). In addition, complete disappearance of peaks associated with Na ion in samples that were exchanged with metal salts indicates complete displacement of Na with a new metal ion. To alleviate concerns that some (or all) of the exchanging metal ions may be present as mechanically trapped chloride salts, as opposed to ionically bonded to carboxylate ions, all samples were scanned for presence of chloride. There were no peaks observed in the spectral range corresponding to chloride binding energy (198.5 eV), indicating that the metal ions are indeed present as ionically bonded entities and are no longer in the form of chloride salts.

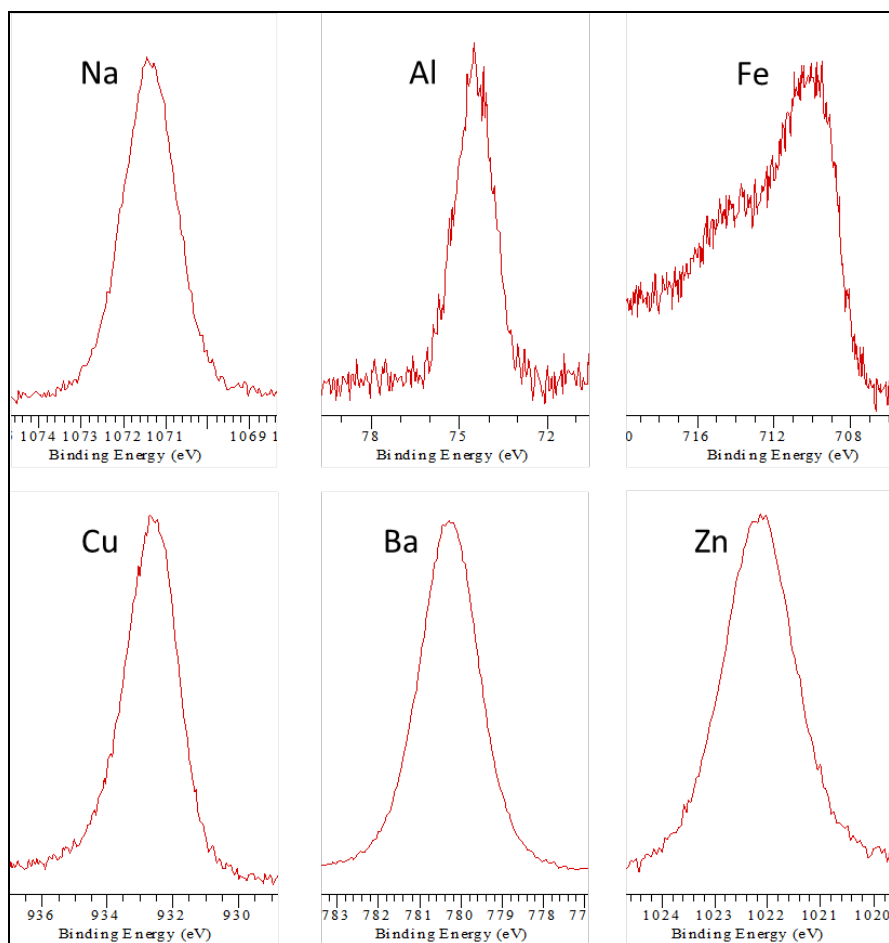


Fig. 8 Selected XPS spectra of regions associated with metals of interest

In a perfect scenario, we would expect concentration of new ions to be proportional to quantity on Na ions in the original film corrected by valence of the new ion. For example, when Na (a +1 ion) is replaced by Al (a +3 ion), the intensity of the Al peak should be 1/3 of the Na one. Unfortunately, low ion concentration and signal intensity resulted in rather poorly defined peaks. This was especially prevalent in cases of Al and Fe, where peaks are barely visible over the background noise. Because of this, any attempts to make a quantitative assessment of concentration of the metallic ions cross-linking the CNF crystals were not reported. (A table of relative signal intensities is provided in the Appendix.)

3.4 Mechanical Properties

As mentioned previously, mechanical properties of original and metal-ion exchanged films were obtained using the MTS Synergie Electromechanical Universal Test System load frame equipped with 50-N load cell and controlled by TestWorks 4.11 software. The summary of the results is shown in Table 2. All

samples exhibited brittle failure behavior. In most cases, elastic modulus values did not change significantly as a function of ion composition when compared to the original unmodified material CNF–Na, which had a baseline value of 3.8 GPa. However, the Cu-ion material (CNF–Cu) modulus increased by 36% to 5.2 GPa. Since the materials exhibit brittle failure mode, the strength of the material (peak stress) was determined by strength at the break point. Even though the scatter of data obtained for each individual material is quite significant, there are clearly differences between the samples as the metallic ions are changed. Average values for Ba and Cu ions show an increase of roughly 15% to 17% in strength, and for Zn a 33% increase over the original material’s 81 MPa value. Surprisingly, Al and Fe exchanged films actually decrease in strength, resulting in a 40% and 60% drop from CNF–Na reference value, respectively. Strain, measured as the elongation at break values for all the materials, was very low, varying from 3% to 1% with original material at 2%. Repeating the behavior observed for strength measurements, strain was compromised when cellulose was exchanged with Al and Fe. Film strength is noticeably improved when Ba or Zn replace the native Na cation, and remains statistically unchanged in the case of Cu due to high levels of scatter in the collected data.

Table 2 Mechanical test results

Sample	Strength		Strain at break		Modulus		Toughness	
	MPa	+ / -	mm/mm	+ / -	GPa	+ / -	MPa	+ / -
CNF-Na	81.0	12.0	0.022	0.002	3.8	456.2	0.96	0.2
CNF-Ba	92.9	13.1	0.031	0.006	4.4	806.4	1.64	0.5
CNF-Cu	95.0	26.9	0.023	0.008	5.2	785.3	0.97	0.4
CNF-Zn	107.7	21.4	0.030	0.007	4.4	861.8	1.75	0.7
CNF-Fe	32.0	7.7	0.009	0.002	3.7	346.5	0.17	0.1
CNF-AL	48.3	20.0	0.014	0.007	4.0	442.0	0.28	0.2

Toughness of the material is a measure of the energy a sample can absorb before it fails and is determined by the area under the stress–strain curve. Material toughness follows a similar trend to the one observed strain, exhibiting a significant decrease in the case of Al and Fe (70% and 80% drop, respectively), comparable values for Cu, and a substantial increase for Ba and Zn (70% and 80% increase, respectively).

Mechanical properties’ evaluation of these samples provides a glimpse into a trend that may be useful for selecting additional metal ion candidates for ionic cross-linking. A pattern emerges when all these results are combined in Fig. 9, with the data points color-coded by valence value: blue is +1, green is +2, and red is +3.

Ionic exchange with Fe and Al consistently results in deterioration of mechanical properties as compared to the original (Na) material. At the same time, Ba, Cu, and Zn show improvement, or at least are statistically equivalent to Na. While it would be premature to propose a conclusive theory regarding the specific reasons for the difference in the behavior, the divalent nature of the metal ions seems to show improvement in mechanical properties. Even though other atomic properties such as electronegativity, atomic radius, and ionization potential vary significantly within this subset, the overall performance still reflects positive direction. At the same time, many of the atomic properties are very similar to the atoms from the second set (Fe^{3+} and Al^{3+}), yet those films exhibit decreased mechanical properties. At this point, it seems the valence of exchanging ions provides the crucial effect in the difference of final properties for these materials. Possibly, trivalent ions (Al and Fe) easily reach the embrittlement with the added third cross-link per ion (increased cross-link density).

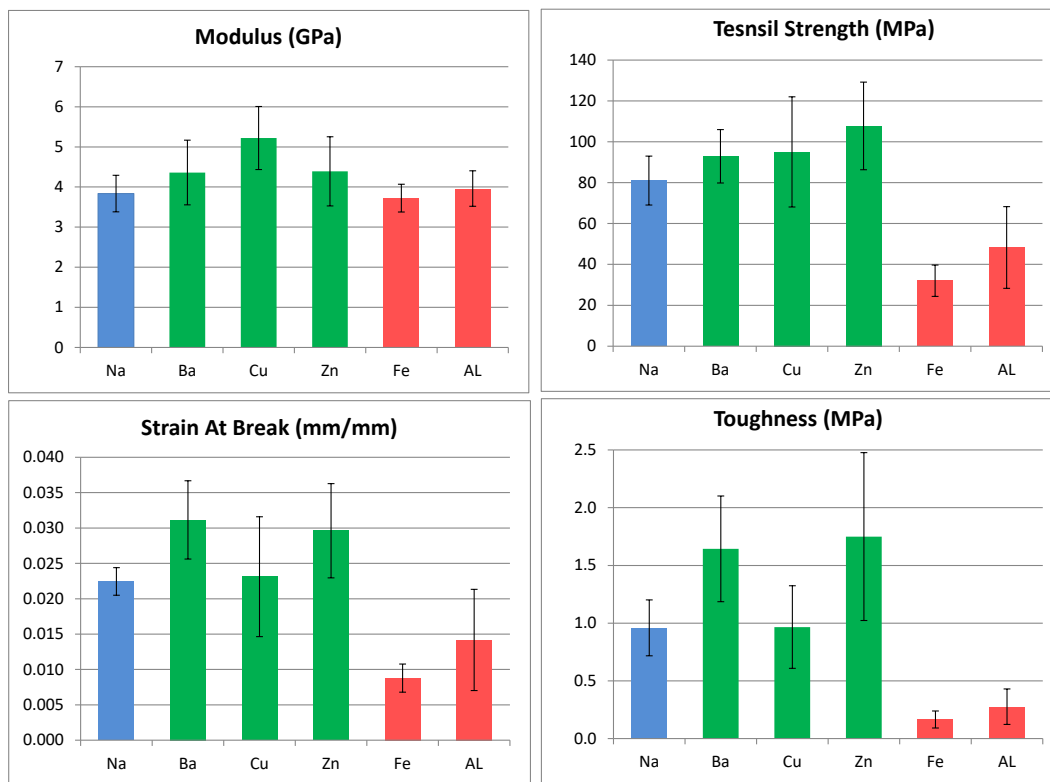


Fig. 9 Bar-graph representation of mechanical data. Metal valence is color-coded as blue = +1, green = +2, and red = +3.

On the other hand, the embrittlement of the films could also be an effect of significantly different ionic radii (Na^{1+} ~116 pm, Ba^{2+} ~149, Cu^{2+} ~87, Zn^{2+} ~88, Fe^{3+} ~69, and Al^{3+} ~68). Differences on this scale may result in large steric hindrance for the +3 ions, where it is difficult for counterions attached to the

saccharide backbone to gather around the small cation as would be required to provide complete ionic cross-link. It could be revealing to evaluate properties of CNF film exchanges with a series of trivalent cations of progressively increasing ion radii and see if toughness and tensile strength could be improved by this method.

When comparing the mechanical property data reported here to the literature,^{15–18} others reported significantly higher tensile strength and moduli. Some of these discrepancies could be results from the use of solid films versus nano-paper,^{17,18} however, while others from the Isogai group^{15,16} used films very similar to ours. They measured mechanical properties of monolithic CNF films exchanged with Na, Al, and Fe ions to have tensile strength between 200 and 250 MPa, and Young's modulus between 12 and 18 GPa. In addition, we measured strain at break values for our films at least 50% lower. Two most probable causes of this discrepancy may be the manufacturing process or the drying procedure. The Isogai group used the process of TEMPO oxidation of the fibers, where the starting CNF material was used as received from the manufacturer in this report. Secondly, the Isogai group dried their films directly from water, while methanol was used to dehydrate the films reported here. Both of these differences could explain the material properties' discrepancies but further evaluation into starting material and sample preparation is needed.

4. Conclusions

In this work, freestanding CNF film containing large quantities of nanocrystals (~70%) was ionically cross-linked in aqueous media using chlorinated metal salts. Metal ions Ba²⁺, Cu²⁺, Zn²⁺, Fe³⁺, and Al³⁺ were used to replace Na ions present on the surface of the nanocrystals and fibrils and to create ionic cross-links to provide positive enhancement of mechanical properties. XPS was used to verify ionic exchange by monitoring the disappearance of the Na ion and presence of new metals in the film after the exchange procedure. TGA of the newly exchanged films did not show significant changes to onset of thermal degradation in nitrogen atmosphere as compared to the original. However, there was a noticeable shift in main degradation temperature. Mechanical properties of the original (Na form) and ionically cross-linked (Ba, Cu, Zn, Fe, and Al) films were determined based on tensile testing. Tensile testing data of the films showed a big discontinuity when comparing the effects of divalent and trivalent metal cations.

Tensile strength, strain at break, and toughness show significant increases when exchanged with divalent cations. Ba or Zn in certain cases provide 30% to 80% increase in these properties, while Cu remained statistically unchanged as

compared to the original Na sample. Trivalent cations (Al and Fe) on the other hand all show significant decreases in these properties.

Modulus remained relatively unchanged, with only Cu (CNF-Cu) showing a significant difference from original material (36% increase). At this point, it seems that the valence of exchanging ions provides the crucial effect in the difference of final properties for these films. Possibly, trivalent ions (Al and Fe) result in embrittlement due to the added third cross-link per ion—effectively increasing cross-link density.

Compilation of these results may provide valuable guidance in selection of potential metal ions for cross-linking CNC-containing films to influence mechanical properties.

5. References

1. Martínez-Sanz M, Lopez-Rubio A, Lagaron JM. Optimization of the nanofabrication by acid hydrolysis of bacterial cellulose nanowhiskers. *Carbohydr Polym.* 2011;85(1):228–236.
2. Freire CSR, Silvestre AJD, Gandini A, Neto CP. New materials from cellulose fibers: a contribution to the implementation of the integrated biorefinery concept. *O Papel.* 2011;72(9):91–96.
3. Habibi Y, Lucia LA, Rojas OJ. Cellulose nanocrystals: chemistry, self-assembly, and applications. *Chem Rev.* 2010;110(6):3479–3500.
4. Habibi Y. Key advances in the chemical modification of nanocelluloses. *Chem Soc Rev.* 2014;43(5):1519–1542.
5. Li Q, Rennecker S. Supramolecular structure characterization of molecularly thin cellulose I nanoparticles. *Biomacromolecules.* 2011;12(3):650–659.
6. Dong H, Snyder JF, Williams KS, Andzelm JW. Cation-induced hydrogels of cellulose nanofibrils with tunable moduli. *Biomacromolecules.* 2013;14(9):3338–3345.
7. Eichhorn SJ, Dufresne A, Aranguren M, Marcovich NE, Capadona JR, Rowan SJ, Weder C, Thielemans W, Roman M, Rennecker S, et al. Review: current international research into cellulose nanofibres and nanocomposites. *J Mater Sci.* 2010;45(1):1–33.
8. Lin N, Huang J, Chang PR, Feng J, Yu J. Surface acetylation of cellulose nanocrystal and its reinforcing function in poly(lactic acid). *Carbohydr Polym.* 2011;83(4):1834–1842.
9. Jung YH, Chang T-H, Zhang H, Yao C, Zheng Q, Yang VW, Mi H, Kim M, Cho SJ, Park D-W, et al. High-performance green flexible electronics based on biodegradable cellulose nanofibril paper. *Nat Comm.* 2015;6:7170.
10. Dong H, Snyder JF, Tran DT, Leadore JL. Hydrogel, aerogel and film of cellulose nanofibrils functionalized with silver nanoparticles. *Carbohydr Polym.* 2013;95(2):760–767.
11. Silverstein RM, Bassler GC, Morrill TC. Spectrometric identification of organic compounds. 5th ed. John Wiley & Sons Inc; 1991.

12. McAllister MJ, Li J-L, Adamson DH, Schniepp HC, Abdala AA, Liu J, Herrera-Alonso M, Milius DL, Car R, Prud'homme RK, et al. Single sheet functionalized graphene by oxidation and thermal expansion of graphite. *Chem Mater*. 2007;19(18):4396–4404.
13. Papageorgiou SK, Kouvelos EP, Favvas EP, Sapalidis AA, Romanos GE, Katsaros FK. Metal-carboxylate interactions in metal-alginate complexes studied with FTIR spectroscopy. *Carbohydr Res*. 2010;345(4):469–473.
14. Max J-J, Chapados C. Infrared spectroscopy of aqueous carboxylic acids: comparison between different acids and their salts. *J Phys Chem A*. 2004;108(16):3324–3337.
15. Shimizu M, Saito T, Isogai A. Water-resistant and high oxygen-barrier nanocellulose films with interfibrillar cross-linkages formed through multivalent metal ions. *J Membrane Sci*. 2016;500:1–7.
16. Isogai A, Saito T, Fukuzumi H. TEMPO-oxidized cellulose nanofibers. *Nanoscale*. 2011;3:71–85.
17. Benítez AJ, Torres-Rendon J, Poutanen M, Walther A. Humidity and multiscale structure govern mechanical properties and deformation modes in films of native cellulose nanofibrils. *Biomacromolecules*. 2013;14(12):4497–4506.
18. Benítez AJ, Walther A. Counterion size and nature control structural and mechanical response in cellulose nanofibril nanopapers. *Biomacromolecules*. 2017;18(5):1642–1653.

Appendix. Relative Signal Intensities

Table A-1 Relative atomistic concentration of various ion-exchanged cellulose nanofibril (CNF) membranes calculated based on average of collected X-ray photoelectron spectroscopy runs

Sample	% C	% O	% M⁺
CNF-Na	58	39	2.5
CNF-Ba	62	37	1.0
CNF-Cu	58	40	1.4
CMF-Zn	61	37	1.1
CNF-Fe	58	40	1.2
CNF-Al	57	42	0.7

Note: C = carbon; O = oxygen; M⁺ = metal ion.

List of Symbols, Abbreviations, and Acronyms

Al	aluminum
ARL	Army Research Laboratory
at.%	atomic percent
Ba	barium
Cl	chlorine
CMF	cellulose microfibril
CNC	cellulose nanocrystal
CNF	cellulose nanofibril
CO ₂	carbon dioxide
COOH	carboxyl group
Cu	copper
DEVCOM	US Army Combat Capabilities Development Command
Fe	iron
FTIR	Fourier transform infrared spectroscopy
H	hydrogen
He	helium
HPLC	high-performance liquid chromatography
mol%	mole percent
Na	sodium
TGA	thermogravimetric analysis
USDA	US Department of Agriculture
wt%	weight-percent
XPS	X-ray photoelectron spectroscopy
Zn	zinc

1 DEFENSE TECHNICAL
(PDF) INFORMATION CTR
DTIC OCA

1 DEVCOM ARL
(PDF) FCDD RLD DCI
TECH LIB

4 DEVCOM ARL
(PDF) FCDD RLW MG
E NAPADENSKY
J A ORLICKI
FCDD RLW MC
J F SNYDER
FCDD RLW BA
H DONG